Clays and Clay Minerals, Vol. 52, No. 4, 411–420, 2004.

ELECTRICAL CONDUCTIVITY SPECTRA OF SMECTITES AS INFLUENCED BY SATURATING CATION AND HUMIDITY

SALLY D. LOGSDON* AND DAVID A. LAIRD

National Soil Tilth Laboratory, 2150 Pammel Drive, Ames, IA 50011, USA

Abstract—Electrical conductivity is an important soil property related to salinity, and is often used for delineating other soil properties. The purpose of this study was to examine the influence of smectite properties on the complex electrical conductivity spectra of hydrated smectitic clays. Four smectites were saturated with Ca, Mg, Na or K and equilibrated at four relative humidities ranging from 56 to 99%. X-ray diffraction was used to determine fractions of the various smectite layer hydrates (0 to 4 layers of interlayer water molecules) in each sample. A vector network analyzer was used to determine the real component of the complex electrical conductivity spectra (σ') for frequencies (f) ranging from 300 kHz to 3 GHz. Values of the dc electrical conductivity (σ_0), the frequency where the slope changes in the spectra (f_r), and the slope at the high-frequency end of the spectra (n) were determined by fitting σ' to $\sigma'(f) = \sigma_0(1 + f/f_r)^n$. Both σ_0 and f_r increased with the total amount of water, the amount of interlayer water, and, for saturating cations in the order K < Mg < Ca < Na. The opposite trends were observed for n. The values of these parameters were influenced by the type of smectite, but the trends were not consistent for the effect of layer charge. The results indicate that interlayer water in smectites contributes to the electrical conductivity of hydrated smectites, and that polarization of water by local electrical fields has a substantial influence on the complex electrical conductivity spectra of smectites. The accuracy of salinity estimates for soils and sediments that are based on conductivity measurements may be adversely affected unless the effects of hydrated clays on electrical conductivity are considered.

Key Words—Bound Water, Charge Carrier, Electrical Conductivity, Hydration, Smectite

INTRODUCTION

Electrical conductivity spectroscopy, the study of the relationship between ac electrical conductivity and frequency, is widely used in materials science for characterizing dielectrics and semiconductors. In soil science, dc electrical conductivity is used to determine soil salinity and measurements of soil dielectric properties are used to determine soil moisture.

Electrical conductivity is increasingly measured indirectly, *in situ* (Hendrickx *et al*., 2002). The standard technique has been the four-electrode Wenner device, but in recent years, time domain reflectometry (TDR) has been used to measure electrical conductivity as well as water content. The salinity of soil solutions is often assumed to be the major contributor to the measured electrical conductivity. Nadler (1998, 1999) showed that hydrated clays also influence the *in situ* electrical conductivity of soils.

Relatively high dc electrical conductivity values have been reported (up to 0.2 S m^{-1}) for hydrated clays and soils (Saarenketo, 1998; Logsdon, 2000; Ishida *et al*., 2000; Logsdon and Laird, 2002), but in contrast, dehydrated clays are non-conducting. The frequency-dependence of the real component of electrical conductivity for hydrated clays and soils has rarely been reported in the literature.

* E-mail address of corresponding author:
logsdon@nstl.gov
DOI: 10.1346/CCMN.2004.0520402

Recent interest in electrical conductivity has arisen because of the effect on soil water content values determined by TDR (Persson and Berndtsson, 1998; Logsdon, 2000; Robinson *et al*., 2003). Electrical conductivity complicates waveform analysis for determining the apparent permittivity. Electrical conductivity also contributes to the frequency-dependent imaginary component of permittivity, which increases the apparent permittivity at lower frequencies. These factors adversely affect the accuracy of soil water-content values determined by TDR.

The complex electrical conductivity (σ^*) of a material has both real (σ') and imaginary (σ'') components. Both the real and imaginary components of the complex electrical conductivity of disordered solids such as ionic glasses, semi-conductors, viscous liquids, humidified sands and other porous media have been shown to be frequency-dependent. Generally, both the dc electrical conductivity and the real component of the complex electrical conductivity are due to the movement and/or reorientation of charge carriers (Dyre, 1988, 1991). The frequency dependence of the complex electrical conductivity is caused by differences in the time scales at which different charge carriers contribute to the movement of current.

Three frequency regions have been discussed for the real component of the electrical conductivity spectra of disordered solids (Long, 1991; Funke, 1994; Hunt, 2001): (1) in the low-frequency region, all dipoles are fully oriented by the external electrical field, hence

electrical conduction is due to the movement of mobile charge carriers (ions and charged particles). In the low-frequency region, the real component of the electrical conductivity is nearly constant. (2) In the mid-frequency region, mobile charge carriers are restricted to hopping between multiple sites and local charge carriers (*e.g.* dipole rotations) start to make a contribution to conduction. In the mid-frequency region, conduction increases non-linearly with frequency. (3) In the high-frequency region, the movement of mobile charge carriers is further restricted to hopping between paired sites and local charge carriers become increasingly important. In the high-frequency region, there is a linear increase in conduction with frequency. Even though the general characteristics of the electrical conductivity spectra of various disordered media are similar, specific characteristics of spectra depend on the nature and properties of the material (Dyre, 1988). Dyre (1991) pointed out that the frequency-dependence of the real component of the complex electrical conductivity indicates that the hopping network is either non-random, inhomogeneous or anisotropic. However, it is not possible to determine from electrical conductivity spectroscopy whether charge-site inhomogeneities are at a macroscopic or microscopic scale (Zvyagin and Keiper, 2001).

The hopping charge carriers in smectites are probably protons associated with surface water molecules and the exchangeable cations residing in smectite interlayers near surface-charge sites (Jonscher, 1978; Dissado and Hill, 1984; Anis and Jonscher, 1993; Logsdon and Laird, 2003). Fripiat *et al*. (1965) and Calvet (1975) provided strong evidence that for humidified smectites, electrical conductivity is due to proton hopping in interlayer water rather than movement of exchangeable cations. Rearrangement of hydrogen bonds and dipole orientations of surface-water molecules contribute to charge transfer for smectites in an electrical field. However, the interlayer environment of smectites is very different from that of a bulk solution. In the interlayers, local electrical fields both strongly polarize water molecules and restrict the mobility of the exchangeable cations. Therefore, we hypothesize that smectite properties, including layer-charge density and the extent of crystalline swelling, influence the complex electrical conductivity spectra of hydrated smectites.

The purpose of this study was to examine statistically the influence of smectite properties on the electrical conductivity spectra of hydrated smectitic clays at room temperature. We attempt to relate the specific characteristics of spectra for the real component of the complex electrical conductivity to variations in the composition and moisture content of the studied smectites. We anticipate that greater understanding of these basic processes will lead to improved interpretation of *in situ* electrical conductivity measurements for soils and sediments.

MATERIALS AND METHODS

The four smectites chosen for this study have different surface-charge densities and proportions of tetrahedral and octahedral charge (Table 1). Hectorite (SHCa-1) from San Bernardino County, California, was supplied by The Source Clays Repository of The Clay Minerals Society, hosted by Purdue University in Indiana. The SPV Bentonite is a Wyoming bentonite supplied by Bariod Division National Lead Co., Houston, Texas. Otay was collected from an exposure in San Diego County, California. The IMV Bentonite was supplied by IMV Div. Floridin Co., Amargosa Valley, Nevada. The raw clay ores were dispersed in deionized water by stirring, and the clay fractions (<2 μm equivalent spherical diameter) were separated by sedimentation. The clay fractions were washed three times with 1 M chloride solutions of $CaCl_2$, $MgCl_2$, NaCl or KCl, dialyzed against deionized water and freeze dried.

Water was added to the samples only through humidification. To do so, the prepared clay samples were equilibrated over distilled water (close to 100% RH) for two weeks. Part of each sample was analyzed, and then subsamples of the humidified clays were equilibrated for an additional 2 weeks over saturated solutions of $ZnSO_4$, NH_4Cl or $Mg(NO_3)_2$ which controlled the RH of the systems at 85%, 74% or 56%, respectively.

ELECTRICAL SPECTROSCOPY MEASUREMENTS AND CALCULATIONS

After equilibration at each RH, duplicate samples were tightly packed into a coaxial cell, similar to the cell described by Lawrence *et al*. (1989) except scaled down in size (Figure 1). When packing densities varied excessively between duplicates, a third sample was prepared and measured. After the humidified clay was packed into the cell, the cell was sealed to prevent loss of water during measurement.

A vector network analyzer (Agilent 8753E) was used to determine complex scattering parameters (S_{11}) for a range of frequencies. Reflection measurements were used to determine the S_{11} values because the sample cell

Table 1. Properties of the studied smectites.

Clay	CEC[1] $cmol_c\ kg^{-1}$	SCD[2] $\mu\ mol_c\ g^{-1}$	SA[3] $m^2\ g^{-1}$	TC[4] %
Hectorite	88	1.20	751	0
SPV Bentonite	96	1.28	752	8
Otay	109	2.11	584	26
IMV Bentonite	122	1.70	752	20

[1] CEC: cation exchange capacity
[2] SCD: surface charge density
[3] SA: specific surface area
[4] TC: tetrahedral charge

https://doi.org/10.1346/CCMN.2004.0520402 Published online by Cambridge University Press

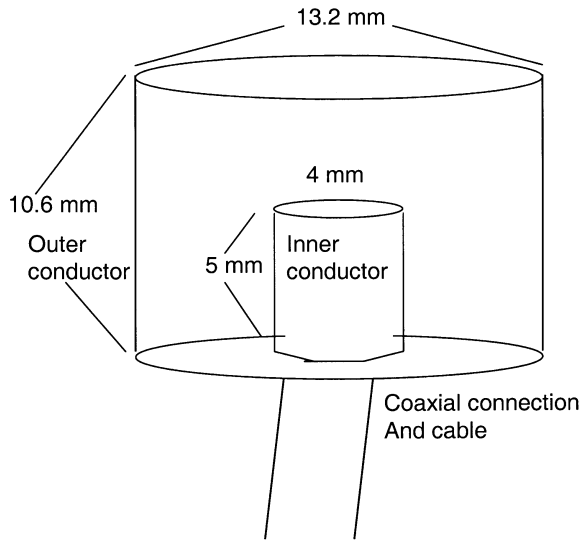

Figure 1. Diagram of a truncated coaxial sample chamber showing the solid inner conductor and cylindrical outer conductor in which the humidified clay was packed.

was open-ended, and the current was reflected back when it reached the end of the sample. The 11 subscript in S_{11} means that the current starts and ends at the same port of the vector network analyzer. A standard reflection calibration was conducted daily using open-circuit, short-circuit, and 50 ohm load termination, with the measurement plane set to the end of the cable. Each sample was measured at several temperatures between 10 and 35ºC. For each measurement, S_{11} values were determined at 800 frequencies between 300 kHz and 3 GHz.

The complex S_{11} values measured by the vector network analyzer were used to determine complex impedance. The complex impedance was converted to complex electrical conductivity and permittivity (ε^*) as described by Campbell (1990) and Logsdon and Laird (2002). To do so, the electrical length of the sample holder was back-fitted as described by Heimovaara *et al*. (1996). The complex electrical conductivity and the complex permittivity are related (Moynihan, 1994):

$$\varepsilon^* = \varepsilon' - i\varepsilon'' \quad (1)$$

$$\sigma^* = \sigma' + i\sigma'' = i2\pi f\varepsilon_v\varepsilon^* \quad (2)$$

where the $'$ refers to the real component and the $''$ refers to the imaginary component, f is frequency (Hz), and ε_v is the permittivity of a vacuum (8.854×10^{-12} F m^{-1}). For this study, we were primarily concerned with the real component of electrical conductivity, although the imaginary component of electrical conductivity is useful for differentiating electrode polarization (charge buildup on the electrodes that increases low-frequency measurements). Low-frequency dispersion, caused by polarization of the material (Dissado and Hill, 1984), is another potential source of error at low frequencies. We monitored the data for large parallel increases in the real and imaginary components of permittivity, evidence of low-frequency dispersion (Anis and Jonscher, 1993; Logsdon and Laird, 2003). Also, frequencies >500 MHz were not included because spectra for the real component of electrical conductivity started to level off, indicative of saturation.

For this study, only 'room-temperature' data were included, to correspond with the X-ray diffraction (XRD) data which were determined at room temperature, and to emphasize the RH-water volume fraction effect. The room-temperature results were actually the means of the ascending and descending real electrical conductivity spectra at 20 and 25ºC, respectively.

The real component of each electrical conductivity spectrum was fitted to $\sigma'(f) = \sigma_0(1 + f/f_r)^n$ (Jonscher, 1978), where f is the frequency, f_r is the critical frequency at which the slope starts to increase, σ_0 is the dc electrical conductivity, and n is the high-frequency slope of the electrical conductivity spectra. The data were fitted using the NLIN statistical procedure given by SAS (1988), and we selected the Marquardt algorithm.

The equation we used is only one of several possible exponential equations that could have been used to model electrical conductivity spectra (Jonscher, 1996). The exponential equation emphasizes interactions between molecules rather than the viscous movement of independent molecules (Jonscher, 1996). Because of electrode polarization and low-frequency dispersion, the fitted dc electrical conductivity (σ_0) may be higher than the true dc electrical conductivity. Furthermore, the physical significance of σ_0, f_r and n has been questioned (Dyre, 1988, 1991; Moynihan, 1994). We evaluated other possible equations, and found that they either did not fit our data or lacked a unique fit due to numerous parameters. In this study, we considered it appropriate to use a relatively simple empirical equation because the equation generally did a good job of fitting our data and because the equation allowed us to reduce the real component of the electrical conductivity spectra to only three parameters, which could be statistically compared with sample properties.

X-RAY DIFFRACTION

The clay samples were analyzed by XRD to determine the extent of crystalline swelling under the same RH conditions used for the dielectric measurements. To do so, samples of the cation-saturated clays were oriented on glass slides by the paste method (Theissen and Harward, 1962). While the oriented specimens were still wet, they were placed in desiccators above saturated salt solutions to control RH as noted above. The specimens were equilibrated with an atmosphere controlled at the appropriate RH for >30 days before the XRD analysis. For the XRD analysis, the specimens were quickly transferred from the controlled-

https://doi.org/10.1346/CCMN.2004.0520402 Published online by Cambridge University Press

atmosphere desiccators to the sample stage of the goniometer and a plastic housing with mylar windows was immediately placed over the sample. A stream of air controlled at the appropriate RH was blown through tubing that connected to the top of the sample housing directly onto the oriented clay specimen while mounted in the goniometer. The samples were analyzed between 2º and 15º or between 2 and 30º2θ using CuKα radiation for a step size of 0.02º2θ with two steps per second.

The XRD data were used to estimate percentages of each phase and ratios of the interlayer to particle volume. NEWMOD (Reynolds and Reynolds, 1996) was used to compute XRD patterns that were fitted to the measured XRD patterns. The NEWMOD simulations provided estimates of the percentages of each phase for the mixed-layer systems. The *d* spacings were assumed to be 1.25, 1.5, 1.75 and 2.0 nm for smectite phases with one, two, three and four discrete layers of interlayer water molecules, respectively.

Calculations

Elemental analysis of the clay samples was performed by inductively coupled plasma-atomic emission spectroscopy using the suspension nebulization technique (Laird *et al*., 1991). The results for the elemental analysis were used to calculate structural formulae and formula unit masses (F_w) for the studied smectites. Relative interlayer volumes, particle volumes and particle densities were calculated by using F_w and the *b* (in nm) crystallographic dimension previously determined by measuring the 060 XRD reflection for another sample of each smectite. The unit-layer thickness was assumed to be 0.95 nm, thus the particle volume per formula unit (V_P) is

$$V_P = b^2(0.95)/(2*3^{0.5}), \quad (3)$$

and the associated interlayer volume per formula unit (V_I) is

$$V_I = b^2(d - 0.95)/(2*3^{0.5}) \quad (4)$$

where *d* is the measured *d* spacing in nm. Both V_I and V_P are expressed in nm^3. Particle density (ρ_p) was calculated as

$$\rho_p = F_w\ 10^{21}/[Ab^2\ (0.95)/(2*3^{0.5})] \quad (5)$$

where A is Avogadro's number and ρ_p is expressed in g/cm^3.

The bulk volumetric water content (θ_w) was calculated from the known total volume of the conductivity cell (*vol*), gravimetric water content (g_w), oven-dried (190ºC) clay mass (*dw*), and by assuming a water density (ρ_w) of 1 g cm^{-3}

$$\theta_w = g_w \times dw/(vol \times \rho_w) \quad (6)$$

The density of interlayer water associated with the smectites could be <1 g cm^{-3}, because water molecules solvating the interlayer cations may prop open interlayers, leaving empty space between the pillars (Prost, 1998). No information on the actual density of the interlayer water was available for the studied smectites, but low water densities are more likely to be a concern at lower RH (<50% RH) than those used in this study.

The volume fraction of clay was calculated using the calculated particle densities

$$\theta_c = dw/(vol \times \rho_p) \quad (7)$$

The total internal water fraction, based only on the internal water and clay content, was calculated from

$$\theta_{ip} = vr_1 \times 30/125 + vr_2 \times 55/150 + vr_3 \times 80/175 + vr_4 \times 105/200 \quad (8a)$$

where vr_j refers to the measured fractions associated with each interlayer water number (j = 1, 2, 3, 4), and the fractions are the ratio of internal water to basal spacing (Table 2). The internal water fraction based on the total volume is

$$\theta_i = \theta_c \times \theta_{ip}/(1 - \theta_{ip}) \quad (8b)$$

and the external water fraction relative to total volume is

$$\theta_e = \theta_w - \theta_i \quad (8c)$$

The fraction of internal water for each basal spacing relative to total volume is

$$\theta_1 = rv_1 \times \theta_i \times 30/(125 \times \theta_{ip}) \quad (9a)$$
$$\theta_2 = rv_2 \times \theta_i \times 55/(150 \times \theta_{ip}) \quad (9b)$$
$$\theta_3 = rv_3 \times \theta_i \times 80/(175 \times \theta_{ip}) \quad (9c)$$
$$\theta_4 = rv_4 \times \theta_i \times 105/(200 \times \theta_{ip}) \quad (9d)$$

A single term representing the extent of water polarization (H in J mol^{-1} of H_2O) in the clay-cation-water systems was derived

$$H = (CEC \times HE/z + CEC \times C)\rho_b \times G/(\theta_w \rho_w) \quad (10)$$

where *CEC* is the cation exchange capacity in $mol_c\ g^{-1}$ of clay, *HE* is the hydration energy of the saturating cation in J mol^{-1} of cation, *z* is the valence of the cation, *C* is the hydration energy of the surface charge sites in J mol^{-1} of the site, ρ_b is the bulk density of the conductivity cell contents in g clay cm^{-3}, ρ_w is the density of water in g of H_2O/cm^3 of H_2O, and *G* is the molecular weight of water in g of H_2O/mol of H_2O. All of these terms are known constants or were measured for the clay-cation-water systems except *C*, the hydration energy of the surface charge sites. Values of *C* were estimated by

$$C = TC \times J + (1 - TC)K \quad (11)$$

where *TC* is the measured fraction of tetrahedral charge in the clay, *J* is the hydration energy of F^{-1} in J mol^{-1}, and *K* is the hydration energy of Cl^{-1} in J mol^{-1}. Thus the water polarization energy, *H*, is the ratio of the total amount of hydration energy arising from the exchangeable cations and the available surface charge sites to the total water in the sample. Note that both *H* and *C* are

https://doi.org/10.1346/CCMN.2004.0520402 Published online by Cambridge University Press

Table 2. Fractional contribution of individual basal spacings to the overall basal spacings determined by NEWMOD analysis of XRD data.

Ion	*d* spacing	SPV				Otay				Hectorite				IMV			
	nm	99[1]	85	74	56	99	85	74	56	99	85	74	56	99	85	74	56
K	1.0	0.0	0.1	0.35	0.5	0.67	0.73	0.74	0.75	0.58	0.78	0.80	0.85	0.50	0.50	0.50	0.53
	1.25	0.3	0.75	0.65	0.5	0.33	0.27	0.26	0.25	0.42	0.22	0.20	0.15	0.50	0.50	0.50	0.48
	1.5	0.7	0.15	0.0	0.0	0.0	0.0	0.0	0.0	0.0	0.0	0.0	0.0	0.0	0.0	0.0	0.0
Na	1.0	0.0	0.0	0.0	0.05	0.2	0.2	0.2	0.32	0.0	0.0	0.0	0.15	0.0	0.0	0.03	0.05
	1.25	0.0	0.0	0.20	0.95	0.0	0.12	0.32	0.68	0.0	0.0	0.95	0.85	0.0	0.0	0.61	0.90
	1.5	0.0	0.81	0.80	0.0	0.68	0.68	0.48	0.0	0.85	0.95	0.05	0.0	0.68	0.95	0.37	0.05
	1.75	0.03[2]	0.19	0.0	0.0	0.12	0.0	0.0	0.0	0.15	0.05	0.0	0.0	0.29	0.05	0.0	0.0
	2.0	0.0	0.0	0.0	0.0	0.0	0.0	0.0	0.0	0.0	0.0	0.0	0.0	0.03	0.0	0.0	0.0
Ca	1.0	0.0	0.0	0.0	0.0	0.2	0.2	0.2	0.2	0.0	0.0	0.0	0.0	0.0	0.0	0.0	0.0
	1.5	0.35	0.77	0.85	0.9	0.32	0.64	0.72	0.76	0.25	0.7	0.82	0.95	0.43	0.75	0.85	0.92
	1.75	0.30	0.23	0.15	0.1	0.48	0.16	0.08	0.04	0.57	0.3	0.18	0.05	0.5	0.25	0.15	0.08
	2.0	0.35	0.0	0.0	0.0	0.0	0.0	0.0	0.0	0.18	0.0	0.0	0.0	0.07	0.0	0.0	0.0
Mg	1.0	0.0	0.0	0.0	0.0	0.2	0.2	0.2	0.2	0.0	0.0	0.0	0.0	0.0	0.0	0.0	0.0
	1.25	0.0	0.0	0.0	0.0	0.0	0.0	0.0	0.0	0.0	0.0	0.0	0.0	0.0	0.0	0.0	0.01
	1.5	0.13	0.7	0.85	0.9	0.28	0.56	0.64	0.74	0.27	0.7	0.75	0.95	0.23	0.75	0.85	0.99
	1.75	0.58	0.3	0.15	0.1	0.52	0.24	0.16	0.06	0.43	0.3	0.25	0.05	0.71	0.25	0.15	0.0
	2.0	0.30	0.0	0.0	0.0	0.0	0.0	0.0	0.0	0.3	0.0	0.0	0.0	0.06	0.0	0.0	0.0

[1] The numbers associated with the clays indicate relative humidity (%)
[2] Na SPV99 had 0.33 at 3.2 nm, 0.3 at 3.6 nm, and 0.33 at 4.2 nm

negative. The hydration energies used in the calculations (*HE, C, J* and *K*) were taken from Bohn *et al*. (1979).

We used stepwise multiple regression to identify the relative contributions that bulk volumetric water content, hydration energy, CEC and percent tetrahedral charge made to dc electrical conductivity, frequency at the slope change, and at the high-frequency slope.

RESULTS

Water content and basal spacing

The ability of smectites to swell by imbibing water is well known (MacEwan and Wilson, 1980). The XRD analysis in this study (Table 2) was consistent with previous findings and demonstrated that smectite swelling increased with increased RH, increased hydration energy of the saturating cations, and decreased smectite layer charge. At 99% RH, most (97%) of the Na-SPV bentonite expanded beyond 2.0 nm into the double-layer swelling range. The XRD analyses for all of the other clay-cation-RH systems indicated swelling within the crystalline swelling range (*d* spacings between 1.0 and 2.0 nm). The other Na-saturated clays were dominated by one-layer hydrates at low RH and had increased proportions of two- and three-layer hydrates as RH increased. The K-saturated clays had only zero- and one-layer hydrates, except the K-SPV at high RH, which was dominated by two-layer hydrates. The Ca- and Mg-saturated clays were dominated by two- and three-layer hydrates. As the RH increased from 55 to 99%, the proportion of three-layer hydrates increased from 3.5% (±2.9) to 48.3% (±12.1). A small proportion of four-layer hydrates was observed for the Ca- and Mg-saturated clays at high RH. The Otay smectite was distinguished from the other smectites by having at least 20% of the layers collapsed to 1.0 nm regardless of saturating cation or RH. The presence of non-expanding layers in the Otay smectite was confirmed independently by elemental analysis, which indicated that ~30% of surface charge sites were occupied by non-exchangeable K.

Relative humidity had the biggest effect on bulk volumetric water content and internal water content; however, RH had a small effect on the relative proportions of external water (Table 3). The saturating cation also had a large effect on the bulk volumetric water content of the clays. The bulk volumetric water contents were high for the Ca- and Mg-saturated clays and low for the K-saturated clays. The saturating cation also had a large influence on the relative distribution of internal and external volumetric water contents. Internal water content followed a similar trend to bulk volumetric water content, but external water content was different. The Ca- and Mg-clays had a large proportion of internal water while most of the water in the K-clays was on the external surfaces. Clay type had only a small influence on bulk volumetric water content and the distribution of water between the internal and external surfaces.

Frequency-dependent complex electrical conductivity

Example spectra of the real component of electrical conductivity for several clay-cation systems at high and low bulk volumetric water contents (Figure 2) show different details of the spectra for each sample, but the general shape of the spectra was similar for all samples. Analysis of

https://doi.org/10.1346/CCMN.2004.0520402 Published online by Cambridge University Press

Table 3. Cation, smectite and humidity main effects on bulk total, external and internal volumetric water contents.

	Water content (m^3 m^{-3})			
Relative humidity	99	85	75	56
Total water content	0.386 a[1]	0.275 b	0.236 c	0.195 d
External water content	0.124 a	0.082 b	0.074 b	0.056 c
Internal water content	0.262 a	0.1963b	0.163 c	0.140 d
Cation	Ca	Mg	Na	K
Total water content	0.330 a	0.326 a	0.265 b	0.167 c
External water content	0.067 c	0.064 c	0.090 b	0.113 a
Internal water content	0.263 a	0.262 a	0.175 b	0.054 c
Clay	SPV	Otay	Hectorite	IMV
Total water content	0.270 b	0.240 c	0.269 b	0.310 a
External water content	0.031 c	0.107 a	0.086 b	0.111 a
Internal water content	0.239 a	0.133 d	0.183 c	0.200 b

[1] Means in the same row followed by the same letter are not significantly different at P = 0.05

variance of the clay electrical properties (dc electrical conductivity, the frequency-at-the-slope change, and the high-frequency slope) indicated that the clay type, RH and saturating cation were all highly significant (Table 4). Relative humidity had the largest effect. Both dc electrical conductivity and the frequency-at-the-slope-change increased as RH increased, whereas the high-frequency slope decreased as RH increased. Saturating cation also had a substantial effect on the electrical properties. The Na-saturated clays had the largest values of the dc electrical conductivity and frequency-at-the-slope-change and the K-clays had the lowest values. The trend for the high-frequency slope is the reverse, high values of the high-frequency slope were obtained for the K-clays and low values for the Na-clays. Clay type also had a substantial effect on the electrical properties. The hectorite and IMV clays had higher values of dc electrical conductivity and frequency relative to the SPV and Otay. Clay type had only a small effect on the high-frequency slope. None of these trends, however, was consistent with a layer-charge effect.

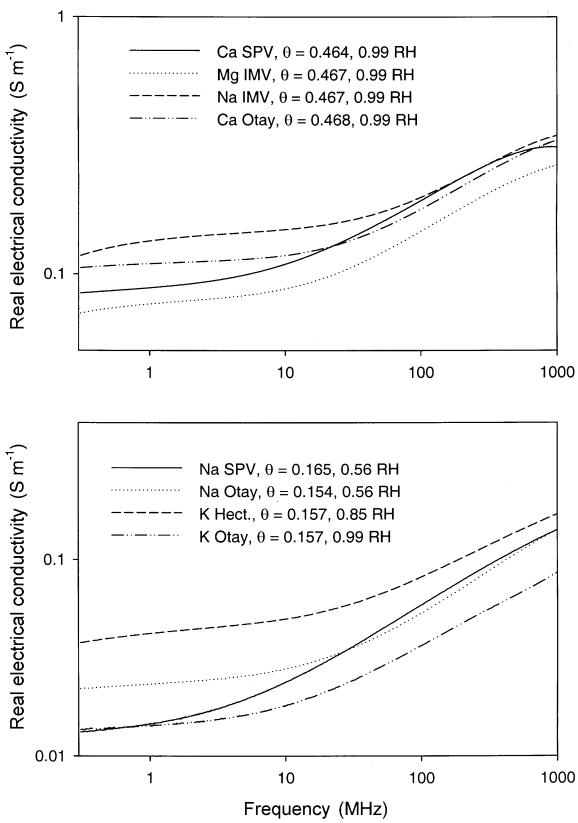

Figure 2. Sample real electrical conductivity spectra at high and low water contents.

The bulk volumetric water content had the strongest correlations with the dc electrical conductivity, and internal water content was somewhat more strongly correlated with dc electrical conductivity than was external water content (Table 5). The results suggest that current was carried both through the interlayers and on the external surfaces of the hydrated clays. Statistical regression models that related electrical properties of the clays to external and internal water content did not improve correlations based on models that only related clay electrical properties to bulk volumetric water content alone. Similarly, models that assigned different contributions to the external water and water in the interlayer hydrates (1 to 4 water molecules thick) did not improve correlations based on models that only related electrical properties to bulk volumetric water content.

Stepwise multiple regression analyses related bulk volumetric water content, cation hydration energy, and CEC and percent tetrahedral charge (%TC) of the clays to the electrical properties (Table 6). In these analyses, the independent variable significance levels were the same in each case even though the regression analyses were conducted independently. For the dc electrical conductivity and the high-frequency slope, only the first three independent variables increased r^2 significantly.

https://doi.org/10.1346/CCMN.2004.0520402 Published online by Cambridge University Press

Table 4. Cation, smectite and humidity main effects on parameters of the real component of electrical conductivity.

	Component			
Relative humidity	99	85	75	56
dc electrical conductivity (mS m^{-1})	80.0 a[1]	44.7 b	27.0 c	12.4 d
Frequency of slope change (MHz)	15.3 a	14.5 a	12.3 b	6.39 c
High-frequency slope	0.328 d	0.361 c	0.404 b	0.454 a
Cation	Ca	Mg	Na	K
dc electrical conductivity (mS m^{-1})	52.2 b	30.4 c	64.9 a	16.9 d
Frequency of slope change (MHz)	12.2 b	8.65 c	20.4 a	7.20 c
High-frequency slope	0.385 b	0.381 b	0.367 c	0.413 a
Clay	SPV	Otay	Hectorite	IMV
dc electrical conductivity (mS m^{-1})	32.6 b	33.6 b	52.4 a	48.0 a
Frequency of slope change (MHz)	3.71 c	11.9 b	16.5 a	17.7 a
High-frequency slope	0.362 c	0.404 a	0.380 b	0.400 a

[1] Means in the same row followed by the same letter are not significantly different at P = 0.05

For the frequency-at-the-slope-change, only the first two independent variables increased r^2 significantly. The water polarization energy, *H*, combines the effects of bulk volumetric water content, cation-hydration energy, CEC, and percent tetrahedral charge into a single variable that represents the ratio of the total clay-cation hydration energy to bulk volumetric water content. The dc electrical conductivity *vs*. water polarization energy plot and the frequency-at-the-slope-change *vs*. water polarization energy plot both had positive log-linear relationships (Figures 3, 4). In contrast, the high-frequency slope *vs*. water polarization energy was a negative linear-linear relationship (Figure 5). The clays had different polarizing energy distribution as a function of the frequency-at-the-slope-change (Figure 4). These results suggest that clay properties that were not accounted for by measured bulk volumetric water content, cation-hydration energy, CEC and percent tetrahedral charge influenced the electrical properties of the clay-cation-water systems.

DISCUSSION AND CONCLUSIONS

Although the shapes of the real component of the complex electrical conductivity spectra were qualitatively similar across all samples (representative spectra are shown Figure 2), the saturating cation, smectite properties and RH had significant effects on fitted components of the spectra (Table 4). These results indicate that smectite properties do have a substantial effect on the real component of the complex electrical conductivity.

Although some features of the spectra for the hydrated smectites were similar to those of disordered solids, there were important distinctions. For the smectites, the high-frequency slope ranged between 0.25 and 0.55 (Figure 5), but literature values for disordered solids range between 0.8 and 1.0 (Dyre, 1988, 1991; Hunt, 2001). This difference is consistent with a greater contribution of mobile charge carriers relative to local charge carriers in the hydrated smectites compared with the disordered solids. In this study, data above 500 MHz were not fitted because the real component of the complex electrical conductivity leveled off at higher frequencies (Figure 2). In contrast, disordered solid spectra (Dyre, 1988; Hunt, 2001) do not level off until 10^{10} or 10^{12} Hz. Hence, the frequency range where the sloping portion of the spectra is apparent was typically one or two orders of magnitude in this study (Figure 2), but it is often four or five orders of magnitude for disordered solids (Hunt, 2001). The reasons for the smaller frequency range observed for the

Table 5. Correlation coefficients (r^2) of internal (Int.), external (Ext.) and total (Tot.) water contents with dc electrical conductivity. Sample number was 134.

	Otay			IMV			Hectorite			SPV		
	Int.[2]	Ext.[3]	Tot.[4]	Int.	Ext.	Tot.	Int.	Ext.	Tot.	Int.	Ext.	Tot.
Mg	.95	.98	.98	.89	.65(1)	.86	.66	ns	.73	.94	ns	.93
Ca	.58	.73	.74	.96	ns	.96	.51	.73	.87	.94	.63	.99
Na	.86	.78	.96	.87	.62	.94	.75	ns	.91	.84	ns	.84
K	.93	.86	.89	.65	.93	.92	.83	.93	.92	.93	.51	.87

[1] ns indicates not significant (P <0.05), [2] Int. is volumetric internal water content, [3] Ext. is volumetric external water content, [4] Tot. is bulk total volumetric water content

https://doi.org/10.1346/CCMN.2004.0520402 Published online by Cambridge University Press

Table 6. Stepwise multiple regression analysis on parameters of the real component of the complex electrical conductivity.

	H_2O	HE[1]	CEC[2]	%TC[3]
dc electrical conductivity				
Adj r^2	0.539*	0.780*	0.794*	0.794ns
Frequency of slope change				
Adj r^2	0.088*	0.226*	0.242ns	0.244ns
High frequency slope				
Adj r^2	0.433*	0.540*	0.639*	0.649ns

[1] HE is hydration energy of the cation (J mol^{-1})
[2] is the cation exchange capacity ($cmol_c$)
[3] %TC is % tetrahedral charge
ns indicates the increase in r^2 was not significant
* indicates significance of p = 0.05

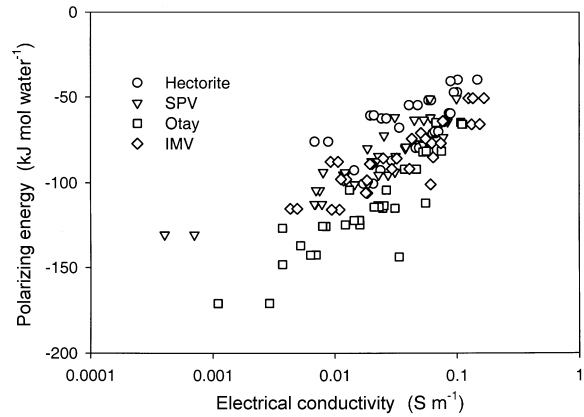

Figure 3. Relationship between water polarizing energy and dc electrical conductivity.

hydrated smectites compared with disordered solids is not clear. However, we speculate that the local charge carriers in disordered solids have greater diversity than is found in the hydrated homo-ionic smectites.

The movement of protons from one water molecule to another is the primary means for electrical conduction in hydrated systems (Jonscher, 1978; Dissado and Hill, 1984; Anis and Jonscher, 1993) and was assumed to be the dominant mechanism for electrical conduction in the hydrated smectite systems. In a dilute aqueous system, the differential movement of charged colloids and counter ions in the diffuse double layers, beyond the shear plane, also contributes to electrical conductivity. In the studied systems, the clays were dialyzed to remove excess counter ions and the bulk volumetric water content was so low that the diffuse double layers collapsed in all of the clays except the Na-SPV at 99% RH. Therefore, it was reasonable to assume that little or no electrophoretic movement of charged colloids occurred in the studied systems. In media with mobile ions other than protons, the ions contribute significantly to the electrical conductivity real-component spectra (Hunt, 2001). However, in the hydrated smectites, the exchangeable cations were bound by electrostatic forces to the negatively charged surface sites, and therefore their mobility was restricted. Although some protons might have displaced the adsorbed cations (as in electrodialysis), the effect would probably be small in an alternating field.

Local charge carriers are believed to contribute substantially to the electrical properties of materials at high frequencies. Water molecules are the most important local charge carriers in the hydrated smectite systems. Because water molecules are dipoles, their dipole moments rapidly reorient in an alternating electrical field. Clay domains might also serve as local charge carriers. Non-bridging *M*>OH groups on lateral edges of clay layers carry a partial charge which depends on the coordination number and valence of the structural metal cation (*M*) as well as the pH of the system. When *M* is Fe^{3+} or Al^{3+}, the non-bridging edge groups may carry either a partial negative charge (*M*>$OH^{-½}$) or a partial positive charge when protonated (*M*>$OH_2^{+½}$). Thus, in an alternating electrical field, a clay domain may act as a local charge carrier due to proton flux from one end of the clay domain to the other. The permanent

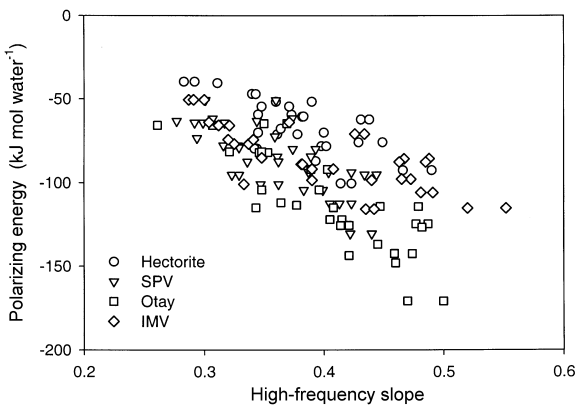

Figure 4. Relationship between water polarizing energy and the critical transition frequency.

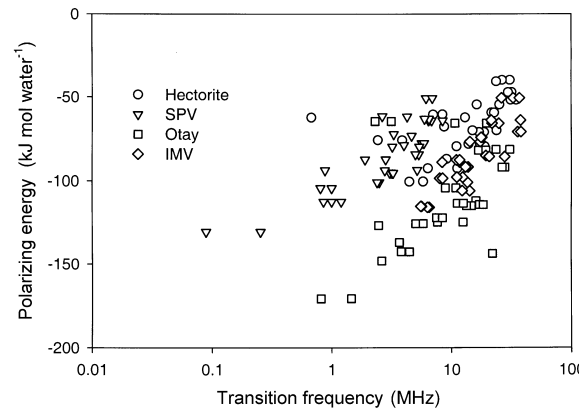

Figure 5. Relationship between water polarizing energy and the high-frequency slope.

https://doi.org/10.1346/CCMN.2004.0520402 Published online by Cambridge University Press

charge sites on basal surfaces of smectites are immobile because their locations are dictated by isomorphous substitution in the crystal structure of the clay. On the other hand, the location of the hydrated interlayer cations is governed by both local and external electrical fields. Although the local electrical field near permanent-charge sites on basal surfaces of the smectites was substantially stronger than the external field imposed by the vector network analyzer, the exchangeable cations could have made minor shifts in position in response to changes in the external field. The primary influence of the surface-charge sites and the exchangeable cations on electrical properties of the hydrated smectite systems was due to the polarization of the interlayer water. The polarization of water molecules by a local electrical environment restricts both proton mobility and the ability of the water molecule dipoles to reorient when an external electrical field is applied.

At low frequencies, local charge carriers, such as water molecule dipoles and polarizable colloidal domains were completely utilized, and therefore made a negligible contribution to the real component of electrical conductivity. Therefore, we assume that dc electrical conductivity was largely determined by proton mobility. The primary factors limiting proton mobility are the extent to which the water molecules are polarized by local electrical fields and tortuosity of the path. Figure 3 provides evidence that the extent of water polarization was a major factor influencing dc electrical conductivity. Although all four of the clays show an increase in dc electrical conductivity with decreasing water polarization energy (Figure 3), the slope is different for each smectite (Otay > IMV = SPV > Hectorite). The different slopes probably reflect the influence of particle morphology on tortuosity and connectivity of the bound water films.

The frequency where the slope of the real component of the complex electrical conductivity changes was highly influenced by clay properties other then CEC and percent tetrahedral charge (Table 4, Figure 4). At this frequency, local charge carriers become increasingly important, suggesting that this frequency represents the time scale in which bound water dipole rotation as well as polarization of clay domains have the greatest influence on the electrical-conductivity real-component spectra. High-resolution scanning electron microscopy (Wu, 2000) provides evidence that individual 2:1 layers of the SPV smectite are substantially larger in lateral dimensions than those of the other clays. This might explain why the average frequency at the slope change was substantially lower for SPV than the other clays (Table 4) and why the SPV data points had a separate distribution from the other clays in Figure 4.

The response of the high-frequency slope to bulk volumetric water content and clay properties (Table 4) and to the water polarization energy (Figure 5) was opposite to that observed for dc electrical conductivity and the frequency-at-the-slope-change. To a substantial extent, this trend was driven by the bulk volumetric water content. The high-frequency slope was a measure of the relative importance of local charge carriers to mobile charge carriers. At low bulk volumetric water contents and when the water was highly polarized by local electrical fields, local charge carriers were relatively more important than mobile charge carriers.

Hydrated smectites and associated exchangeable cations can have a large dc electrical conductivity. When smectites are a significant component of soils or sediments, the bulk dc electrical conductivity will be influenced by the smectite conductivity as well as the solution conductivity. The accuracy of salinity estimates based on dc electrical conductivity measurements for soils and sediments will be adversely affected unless the effects of hydrated clays on electrical conductivity are considered. Furthermore, the results of this study demonstrate that electrical conductivity spectroscopy has the potential to provide information about the nature and properties of hydrated smectites.

REFERENCES

Anis, M.K. and Jonscher, A.K. (1993) Frequency and time-domain measurements on humid sand and soil. *Journal of Materials Science*, **28**, 3626–3634.

Bohn, H.L., McNeal, B.L. and O'Connor, G.A. (1979) *Soil Chemistry*. John Wiley and Sons, New York.

Calvet, R. (1975) Dielectric properties of montmorillonites saturated by divalent cations. *Clays and Clay Minerals*, **23**, 257–265.

Campbell, J.E. (1990) Dielectric properties and influence of conductance in soils at one to fifty megahertz. *Soil Science Society of America Journal*, **54**, 332–341.

Dissado, L.A. and Hill, R.M. (1984) Anomalous low-frequency dispersion. *Journal of the Chemical Society Faraday Transactions 2*, **80**, 291–319.

Dyre, J.C. (1988) The random free-energy barrier model for ac conduction in disordered solids. *Journal of Applied Physics*, **64**, 2456–2468.

Dyre, J.C. (1991) Some remarks on ac conduction in disordered solids. *Journal of Non-Crystalline Solids*, **135**, 219–226.

Fripiat, J.J., Jelli, A., Poncelet, G. and Andre, J. (1965) Thermodynamic properties of adsorbed water molecules and electrical conduction in montmorillonites and silicas. *Journal of Physical Chemistry*, **69**, 2185–2197.

Funke, K. (1994) Jump relaxation model and coupling model – a comparison. *Journal of Non-Crystalline Solids*, **172–174**, 1215–1221.

Heimovaara, T.J., de Winter, E.J.G., van Loon, W.K.P. and Esveld, D.C. (1996) Frequency-dependent dielectric permittivity from 0 to 1 GHz: Time domain reflectometry measurements compared with frequency domain network analyzer measurements. *Water Resources Research*, **32**, 3603–3610.

Hendrickx, J.M.H., Das, B., Corwin, D.L., Wraith, J.M. and Kachanoski, R.G. (2002) 6.1.4 Indirect measurement of solute concentration. Pp. 1274–1297 in: *Methods of Soil Analysis Part 4: Physical Methods* (J.H. Dane and G.C. Clark, editors). Soil Science Society of America, Inc., Madison, Wisconsin.

Hunt, A.G. (2001) Ac hopping conduction: perspective from

percolation theory. *Philosophical Magazine B*, **81**, 875–913.

Ishida, T., Makino, T. and Wang, C. (2000) Dielectric-relaxation spectroscopy of kaolinite, montmorillonite, allophane, and imogolite under moist conditions. *Clays and Clay Minerals*, **48**, 75–84.

Jonscher, A.K. (1978) Low-frequency dispersion in carrier-dominated dielectrics. *Philosophical Magazine B*, **38**, 587–601.

Jonscher, A.K. (1996) *Universal Relaxation Law*. Chelsea Dielectrics Press, London, 415 pp.

Laird, D.A., Dowdy, R.H. and Munter, R.C. (1991) Suspension nebulization analysis of clays by inductively coupled plasma-atomic emission spectroscopy. *Soil Science Society of America Journal*, **55**, 274–278.

Lawrence, K.C., Nelson, S.O. and Kraszewski, A.W. (1989) Automated system for dielectric properties measurements from 100 kHz to 1 GHz. *Transactions of the American Society of Agricultural Engineers*, **32**, 304–308.

Logsdon, S.D. (2000) Effect of cable length on TDR calibration for high surface area soils. *Soil Science Society of America Journal*, **64**, 54–61.

Logsdon, S.D. and Laird, D.A. (2002) Dielectric spectra of bound water in hydrated Ca-smectite. *Journal of Non-Crystalline Solids*, **305**, 243–246.

Logsdon, S.D. and Laird, D.A. (2003) Ranges of bound water properties associated with a smectite clay. Pp. 101–108 in: *Electromagnetic Wave Interaction with Water and Moist Substances, Proceedings of Conference*, Rotorua, New Zealand.

Long, A.R. (1991) Hopping conductivity in the intermediate frequency regime. Pp. 207–231 in: *Hopping Transport in Solids* (M. Pollak and B. Shklovskii, editors). Elsevier Science Publishers, B.V., Amsterdam, The Netherlands,

MacEwan, D.M.C. and Wilson, M.J. (1980) Interlayer and intercalation complexes of clay minerals. Pp. 197–244 in: *Crystal Structures of Clays and Clay Minerals* (G.W. Brindley G. Brown, editors). Monograph **5**, Mineralogical Society, London.

Moynihan, C.T. (1994) Analysis of electrical relaxation in glasses and melts with large concentrations of mobile ions. *Journal of Non-Crystalline Solids*, **172–174**, 1395–1407.

Nadler, A. (1998) Comments on "Comparison of three methods to calibrate TDR for monitoring solute movement in undisturbed soil". *Soil Science Society of America Journal*, **62**, 489–490.

Nadler, A. (1999) Comments on "Measurement of volumetric water content by TDR in saline soils" by G.C.L. Wyseure. *European Journal of Soil Science*, **50**, 181–183.

Persson, M. and Berndtsson, R. (1998) Texture and electrical conductivity effects on temperature dependency in Time domain reflectometry. *Soil Science Society of America Journal*, **62**, 887–893.

Prost, R., Koutit, T., Benchara, A. and Huard, E. (1998) State and location of water adsorbed on clay minerals: consequences of the hydration and swelling-shrinkage phenomena. *Clays and Clay Minerals*, **46**, 117–131.

Reynolds, R.C. Jr. and Reynolds, R.C. III (1996) *Newmod-for-Windows. The Calculation of One-dimensional X-ray Diffraction Patterns of Mixed-layered Clay Minerals*. Published by the authors, 8 Brook Road, Hanover, New Hampshire 03755.

Robinson, D.A., Jones, S.B., Wraith, J.M., Or, D. and Friedman, S.P. (2003) A review of advances in dielectric and electrical conductivity measurements in soils using time domain reflectometry. *Vadose Zone Journal*, **2**, 444–475.

Saarenketo, T. (1998) Electrical properties of water in clay and silty soils. *Journal of Applied Geophysics*, **40**, 73–88.

SAS (1988) *SAS/STAT User's Guide, Release 6.03 Edition*. SAS Inst. Inc. Cary, NC. 1028 pp.

Theissen, A.A. and Harward, M.E. (1962) A paste method for preparation of slides for clay mineral identification by x-ray diffraction. *Soil Science Society of America Proceedings*, **26**, 90–91.

Wu, J. (2000) *Interactions and Transformations of Chlorpyrifos in Aqueous and Colloidal Systems*. PhD dissertation, Iowa State University.

Zvyagin, I.P. and Keiper, R. (2001) Conduction in granular metals by hopping via virtual states. *Philosophical Magazine B*, **81**, 997–1009.

(*Received 22 May 2003; revised 19 February 2004; Ms. 795; A.E. William F. Jaynes*)